Tuning molecular motor transport through cytoskeletal filament network organization

Journal:	*Soft Matter*
Manuscript ID	SM-ART-09-2019-001904.R1
Article Type:	Paper
Date Submitted by the Author:	21-Jan-2020
Complete List of Authors:	Scholz, Monika; University of Chicago Weirich, Kimberly; University of Chicago Gardel, Margaret; U. of Chicago, Dinner, Aaron; University of Chicago, Chemistry

SCHOLARONE™
Manuscripts

Soft Matter

ARTICLE TYPE

Tuning molecular motor transport through cytoskeletal filament network organization

Monika Scholz,[a,b,e] Kimberly L. Weirich,[a,b] and Margaret L. Gardel [a,b,c] and Aaron R. Dinner[a,b,d,*]

Within cells, crosslinking proteins organize cytoskeletal filaments both temporally and spatially to create dynamic, and structurally diverse networks. Molecular motors move on these networks for both force generation and transport processes. How the transport statistics depend on the network architecture remains poorly characterized. Using cross-linking proteins (α-actinin, fimbrin, fascin, or filamin) and purified actin, we create cytoskeletal networks with diverse microscopic architectures. We track the motion of myosin II motor proteins moving on these networks and calculate transport statistics. We observe that motor dynamics change predictably based on the bundling of filaments within the underlying networks and discuss implications for network function.

Introduction

Diverse physiological functions—including intracellular transport, cellular shape change, and cell motility—center on the cytoskeleton, an assembly of polar semi-flexible filaments, crosslinking proteins, and molecular motors[1]. Distinct microscopic arrangements of these components, ranging from tight bundles and long-range fibers to dense meshes[2] are linked to specific functions. For example, tight bundles support thin, elongated local protusions known as filopodia. These allow cells to directionally probe their mechanical and chemical environments, and initiate directional growth[3]. In contrast, the dynamics of the mesh-like actin cortex drive morphological changes in cell shape, for example during cell division, cell migration, and tissue morphogenesis.

Cytoskeletal structure is determined locally by the densities of the filaments, crosslinking proteins, and motors[4,5], as well as by their specific properties. In particular, crosslinking proteins vary in the extent to which they restrict the geometries of the filaments that they bind. Of importance for the present study, cross-linking proteins bundle filaments in ways that constrain filaments spacing and may enforce the alignment of filament polarities. A positive feedback exists between the local cytoskeletal structure and the recruitment of additional crosslinking proteins[6,7], such that dis-

tinct structures emerge in cells.

Understanding the consequences of different filament arrangements for network mechanics has been the subject of intense investigation[8–14]. One element that is clearly important for the ability to support tension is network percolation[8]. While percolation requires that there be sufficient crosslinkers that the network is well connected, very high crosslinker densities can actually inhibit contractility[8,15]. Moreover, the geometric restrictions of specific crosslinkers impact the deformation modes available to a network and, in turn, both its (visco)elasticity and contractility[5,11,15,16].

While cytoskeletal structure also clearly affects intracellular transport[17,18], the relation between specific filament arrangements and motor motion has received comparatively less attention to date. Filament intersections have been shown to control motor routing in a manner that depends on the dimension of the network[19], the geometry of the participating filaments[20] and their polarity[21]. Furthermore, multiple intersections can give rise to network cycles that trap motors with power-law statistics[22]. Put together, these studies suggest that cells can control transport by modulating the nature and density of intersections in their cytoskeletal networks.

Changing the densities of the participating crosslinking proteins impacts not only the network structure but also the structure within bundles, which can also affect transport[23]. Single motors of myosin X were shown to select unipolar bundles over networks in actin assemblies derived from cells[24]; the transport of single kinesin-1 motors was shown to be influenced by both the polarity and spacing of microtubules in bundles[25]. Such effects appear to depend on the nature of the motors. Single motors can vary in speed, processivity, and polarity preference[26], and assembly into

[a] James Franck Institute, The University of Chicago, Chicago, IL 60637

[b] Institute for Biophysical Dynamics, The University of Chicago, Chicago, IL 60637

[c] Department of Physics, The University of Chicago, Chicago, IL 60637

[d] Department of Chemistry, The University of Chicago, Chicago, IL 60637

[*] dinner@uchicago.edu

[e] Present address: Max Planck Research Group Neural Information Flow, Center of Advanced European Studies and Research (caesar), 53175 Bonn, Germany

‡A preliminary version of this work, doi: https://doi.org/10.1101/277947, was deposited in bioxiv on 6 Mar 2018.

teams can modulate these behaviors and yield new, collective effects[22,27,28]. It was recently reported that bundles enhanced the transport distance in teams of non-processive myosin Vc motors, but not in teams of processive myosin Va motors[29].

These observations point to the need to understand how specific bundling proteins impact transport. To this end, here, we study the dynamics of skeletal muscle myosin II, a non-processive motor which forms assemblies with several hundred motor heads, on biochemically well-defined networks of actin filaments bundled by α-actinin, fimbrin, fascin, or filamin *in vitro*. We characterize both the extent and direction of the motions statistically and show how they can be interpreted in terms of the known features of the crosslinking proteins.

Materials and Methods

Protein and vesicle preparation

Monomeric actin was purified from rabbit skeletal muscle acetone powder (Pel-Freez Biologicals) using a protocol adapted from[30]. For imaging with fluorescence microscopy, actin monomers were labeled with the fluorophore tetramethylrhodamine-6-maleimide (TMR; Life Technologies). Both labeled and unlabeled actin were stored at 4°C in 2 mM Tris, 0.1 mM CaCl$_2$, 1 mM NaN$_3$, 0.5 mM dithiothreitol, and 0.2 mM ATP. All other proteins were stored at -80°C in buffers as follows. Skeletal muscle myosin II was purified from chicken tissue[31], labeled with the fluorophore Alexa-642 maleimide ([32]; Life Technologies) and stored in 600 mM KCl, 10 mM EDTA, and 25 mM KPO$_4$ at pH 6.6. Filamin was purified from chicken gizzard using a protocol adapted from[33] and was stored in 10 mM Tris-HCl, 600 mM KCl, 1 mM dithiothreitol, 1 mM EDTA, 2 mM MgCl$_2$, 0.02 % NaN$_3$, at pH 7.4. Fascin, fimbrin, and α-actinin-4 were gifts of the D. Kovar Laboratory at the University of Chicago. Human fascin was expressed in *E. coli*, purified according to[34], and stored in 20 mM tris-HCl, pH 8.0, 10 vol% glycerol, 100 mM NaCl, 0.2 mM EDTA, 0.01 % NaN$_3$, 1 mM DTT. Yeast (*S. pombe*) fimbrin was purified according to[35] and stored in 20 mM HEPES, 1 mM EDTA, pH 8.0, 200 mM KCl, 0.01% NaN$_3$, 10% glycerol, 1 mM DTT. Human α-actinin-4 was expressed in *E. coli*, purified according to[36], and stored in 20 mM Tris-HCl, pH 7.9, 100 mM NaCl, 0.2 mM EDTA, 0.01% NaN$_3$, 1 mM DTT, and 10% glycerol.

Unilamellar vesicles were prepared by first drying a phospholipid (1,2-dioleoyl-sn-glycero-3-phosphocholine; Avanti Polar Lipids) film under nitrogen gas. The phospholipid film was resuspended in vesicle buffer (10 mM sodium phosphate buffer, pH 7.5, 140 mM sodium chloride) and extruded into unilamellar vesicles at ambient temperature ($\sim$ 20°C, above the phospholipid gel transition temperature) through 200 and 50 nm pore polycarbonate membranes (20 x each in a Liposofast extruder; Avestin) following previously detailed methods[37]. Extruded vesicles were stored at 4° C until use.

Microscopy sample preparation

Networks of bundled actin were polymerized in a thin layer at a surface of a flow cell. A supported lipid bilayer, formed by incubating a UV-ozone cleaned borosilicate coverslip (Fisherbrand)

with 1 mM vesicle suspension for 15 min, passivated the surface. After a complete bilayer formed, excess vesicle suspension was exchanged with actin polymerization buffer (10 mM imidazole, 50 mM KCl, 0.2 mM EGTA pH 7.5, 300 μM ATP). Monomeric actin (2.0 μM unlabeled and 0.64 μM TMR-labeled) was added to initiate the polymerization of long, entangled actin. Depletion agent (0.3 wt %, 15 centipoise methylcellulose, Sigma) crowded actin to the surface. An oxygen scavenging system (50 μM glucose, 0.5 vol % β-mercaptoethanol, glucose oxidase, and catalase) reduced photobleaching. After 30 min of polymerization, crosslinker was added to initiate the formation of actin filaments into a network of bundles. Thick filaments of myosin II were polymerized in a similar manner by adding monomeric myosin II (20 nM) to a separate, actin-free solution. After 10 min of polymerization, myosin in ATP ($\sim$2% of total sample volume) was gently mixed with the solution above the actin network, such that the final concentrations were 3.8 pM myosin and 2.3 mM ATP. Actin and myosin were imaged with a inverted microscope (Nikon Eclipse Ti-PFS) equipped with a spinning disk confocal head (CSUX, Yokogawa), 561 nm and 647 nm laser lines, 60×/1.49 NA oil immersion objective (Zeiss), and a CCD camera (Coolsnap HQ2, Photometrics). Imaging began $\sim$10 min after myosin was added to the sample. Images were collected at 1.5 s (shuttered) intervals or 100 ms (unshuttered, streamed data) intervals. Conditions with slower motor speeds (fimbrin and α-actinin) were imaged at the slower, shuttered intervals. Fascin and filamin resulted in fast motor motion and were collected using unshuttered intervals.

Particle tracking

The image stacks obtained from imaging the motion of myosin II on actin networks were analyzed as follows: Single-particle trajectories were obtained using the Python-based implementation of the Crocker-Grier algorithm Trackpy[38]. The search range for linking was set to be the largest displacement in a dataset that was tracked manually. All other parameters were set to the default values given in Trackpy and are reported in the supplementary materials accompanying[22]. The quality of the resulting myosin trajectories was inspected by overlaying the trajectories on a maximum-projection of the collected microscopy images.

Results

Distinct filament bundles can be reconstituted *in vitro*

To investigate the impact of bundle structure on transport, we generated biochemically well-defined networks *in vitro* by crosslinking actin filaments with individual types of crosslinkers. In each case, we polymerized actin and crowded the resulting filaments to a thin ($\sim$200 nm) layer near a passivated coverslip[39]. Upon adding crosslinker, a network of bundled filaments formed and coarsened over 30 minutes into a configuration that then persisted without significant further change (typical images are shown in gray in Fig. 1). After each network stabilized, we added pre-formed filaments of skeletal muscle myosin II. The myosin concentration was sufficiently low that the motors do not deform the overall network structure, but instead move along the bundles (Fig. 1, pink trajectories).
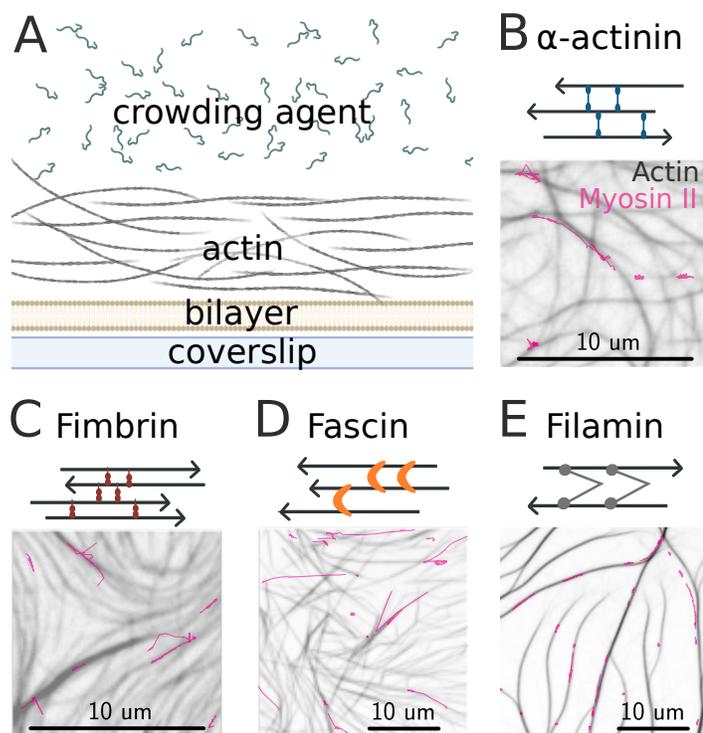
Fig. 1 (A) Cross-section of the experimental preparation. Structures of networks crosslinked by α-actinin (B), fimbrin (C), fascin (D) or filamin (E). Schematics show the expected arrangements of filament polarities, indicated by black arrows. Fluorescence microscopy images are overlaid with myosin II trajectories (pink). Each line represents the trajectory of an individual motor protein. Note that the scale of the images change between panels, due to the large differences in myosin II speeds on different networks.

Transport properties depend on the microscopic bundle architecture

We recorded the motion of the myosin motors on the stable actin networks. Myosin minifilaments, composed of many myosin sub-

units appear as puncta in the recordings and can be tracked using single particle tracking as described in Materials and Methods. The resulting trajectories align well with the crosslinked actin filaments, indicating that the motors are moving along the bundles (Fig. 1). For each crosslinker condition we tracked more than 200 myosin puncta for at least 30 frames of the experiment (see Table). These trajectories were used for all subsequently described analyses, unless otherwise indicated. The trajectories in each condition are from a single preparation of an actin network, which allowed averaging across trajectories without concern about batch effects. The dataset for fimbrin was previously shown in[22].

For each bundle microstructure, we computed the time-averaged mean-squared displacement (TA-MSD) as a function of lag time Δ and measurement time T as previously described[22,45,46]:

$$\langle \overrightarrow{R(T,\Delta)^2} \rangle = \frac{1}{T-\Delta} \int_0^{T-\Delta} [\vec{x}(t+\Delta) - \vec{x}(t)]^2 dt, \qquad (1)$$

where $\vec{x}(t)$ is the position of a motor at time t.

The exponent α in the scaling relation $\langle \overrightarrow{R(T,\Delta)^2} \rangle \propto \Delta^\alpha$ characterizes the motion: $\alpha = 1$ for simple diffusion, and $\alpha = 2$ for a purely directed motion; non-integer values are possible as well (e.g.,[45,46] and references therein). We observe that the exponent of the TA-MSD as a function of lag time changes depending in the underlying bundle structure (Fig. 2). The polarity-sorted bundles created by the crosslinking protein fascin lead to an exponent close to two, indicating strongly directed motion. In contrast, the exponent of the TA-MSD is closer to one for filamin, α-actinin and fimbrin.

We also consider how the TA-MSD varies as a function of measurement time, T. Generally it is unchanging. However, when a continuous spectrum of time scales contributes to the dynamics, the TA-MSD can decrease with a power-law dependence on T. Such a situation has been observed in particle-tracking data for motors[22,22,45–47] and corresponds to the motors experiencing a hierarchy of traps with a distribution of dwell times. We previously described a mechanism that can give rise to such dynamics[22]. The essential idea is that a motor with a high valency can cycle unproductively between filaments that are close in space. As the number of heads that can engage filaments increases, the decrease becomes more pronounced (the magnitude of a negative exponent increases).

The results are presented in Fig. 2B and Table 1. We observe a decrease in the TA-MSD with the measurement time for motors moving on networks crosslinked by α-actinin, consistent with previous results[46]. Similar statistics are obtained for motors moving on networks crosslinked by fimbrin. Both of these proteins generate mixed polarity bundles, with filament spacings ($\sim$8 and 35 nm) that are small in comparison with the sizes of the myosin minifilaments (100-500 nm). We thus interpret the results to indicate that the motors are cycling to similar extents between filaments in these bundles. The decrease in the TA-MSD is somewhat less pronounced for motors moving on networks crosslinked by filamin. This protein is expected to result in a larger filament spacing ($\sim$160 nm), approaching the size of the myosin minifilaments. As a result, fewer heads should be able to engage at a

We constructed bundles using four different crosslinkers: α-actinin, fimbrin, fascin, and filamin. Bundles constructed with α-actinin (Fig. 1 A) are known to be rigid, with mixed polarity actin filaments that pack tightly to form a square lattice with side length $\sim$35 nm within the bundle[6,40,41]. Bundles crosslinked with α-actinin are primarily associated with force producing assemblies such as stress fibers[1]. To create structurally similar bundles with mixed polarity but different spacing, we crosslinked filaments with fimbrin (Fig. 1B), which is known to generate an intrafilament spacing of $\sim$8 nm. Such bundles are associated with cellular assemblies such as microvilli[6,42]. By constructing bundles with the crosslinker fascin (Fig. 1C), we created bundles with similar spacing to the fimbrin bundles, but with aligned actin filament polarity. Bundles crosslinked with fascin are generally associated with cellular assemblies that mediate unidirectional transport such as filopodia[6,43]. Finally, we created looser bundles using low concentrations of the crosslinker filamin (Fig. 1D), which is known to generate an intrafilament distance of $\sim$160 nm[44].

time, and there should be less cycling. Finally, there is little dependence on T in the case of fascin; this is consistent with the idea that trapping is not possible when all the filament polarities in a bundle are the same.
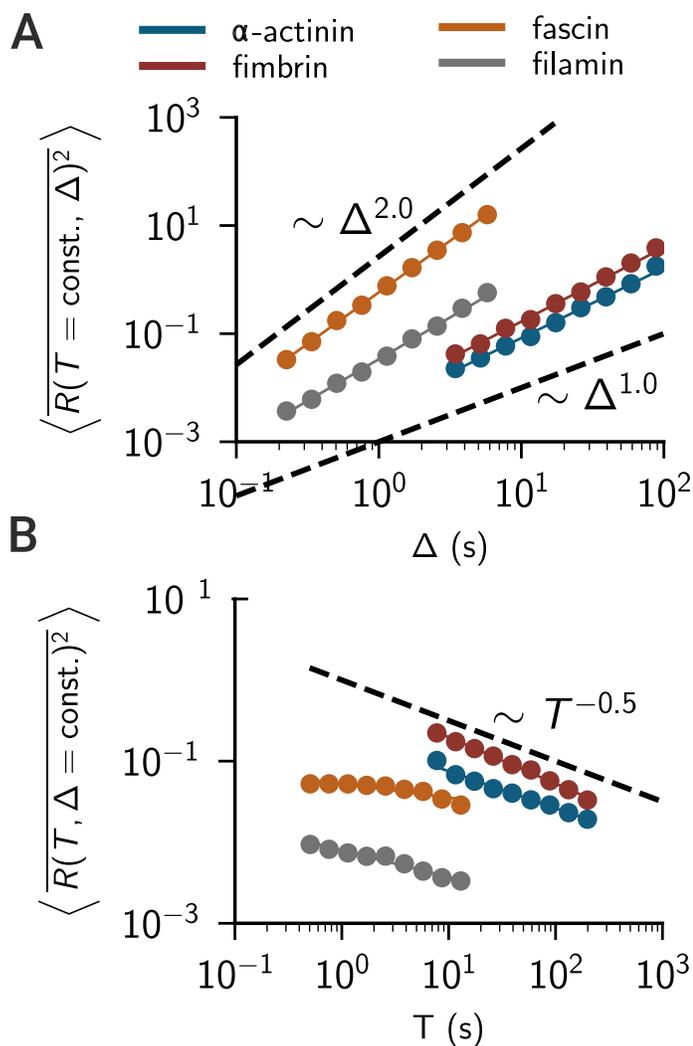
Crosslinker	Number of Trajectories	Exponent $\overline{\langle R(T=const.,\Delta)^2 \rangle}$	Exponent $\overline{\langle R(T,\Delta=const)^2 \rangle}$
α-actinin	210	1.293 ± 0.036	-0.457 ± 0.022
fimbrin	251	1.369 ± 0.034	-0.573 ± 0.018
fascin	236	1.905 ± 0.016	-0.168 ± 0.034
filamin	256	1.543 ± 0.033	-0.329 ± 0.027

Table 1 Exponents of the mean-squared displacement shown in Fig. 2. The error is the statistical error of the fit and represents the 1-σ bounds of the parameter values.

Fig. 2 Mean-squared displacement of myosin II minifilaments on actin networks crosslinked with different proteins (A) as a function of lag time (Δ) and (B) as a function of measurement time (T). $T = 9$ s and $\Delta = 0.2$ s for fascin (orange) and filamin (gray). For α-actinin (blue) and fimbrin (red), $T = 137.7$ s and $\Delta = 3.06$ s. The mean trajectory lengths are 167, 208, 16 and 17 s for α-actinin, fimbrin, fascin and filamin, respectively.

Angular distribution illustrates microscopic directional changes

The TA-MSD cannot reveal directional correlations within trajectories, but there is evidence of such correlations in particle-tracking studies of molecular motors[45–50]. To quantify such correlations, we use the relative angle distribution[46]. The relative angle is defined by

$$\cos\theta(t;\Delta) = \frac{\vec{v}(t;\Delta) \cdot \vec{v}(t+\Delta;\Delta)}{|\vec{v}(t;\Delta)||\vec{v}(t+\Delta;\Delta)|}, \tag{2}$$

where $\vec{v}(t;\Delta) = \vec{x}(t+\Delta) - \vec{x}(t)$. The normalized histogram (probability density function, PDF) of θ values for successive vectors within trajectories can be used as a directional order parameter.

The relative angle distribution is flat for simple diffusion because there are no correlations between steps of the random walk. A dictionary of relative angle distributions for a variety of more complicated transport processes can be found in[46]. Consistent with previous observations for molecular motors[46], for the four experimental conditions that we consider here (Fig. 3), we generally observe peaks at $\theta = 0$ and $\theta = \pi$, indicating an apparently directed motion and frequent reversals, respectively.

The relative angle distribution can be calculated at different Δ to elucidate the timescales contributing to the motion. To investigate the effects on the transport of local structure, as opposed to large-scale network topology, we chose a small Δ ($\Delta = 0.1, 0.1, 1.53, 1.53$ s for fascin, filamin, α-actinin and fimbrin, respectively). To compare recordings of the motion on different crosslinked networks, the magnitude of Δ was chosen to be inversely proportional to the mean motor speed on a given network. For example, the mean speed of myosin on the fimbrin-crosslinked network is only 38 nm/s whereas motors on the fascin-crosslinked network move at 620 nm/s. Thus, the respective values for Δ are 1.53 s and 0.1 s, respectively. We include all trajectories in the analysis, even those that are not moving significantly during our measurement. The average motor speed on fascin bundles, which includes this relatively immobile population, is smaller than the unloaded gliding speed of myosin on actin filaments[51,52].

The motors on the fimbrin-crosslinked network show a strong peak at π, indicating that motors change direction frequently. This is consistent with tight, mixed polarity bundles that create an environment that supports tug-of-war[53,54] and cycling[22] mechanisms. Again the results for α-actinin and fimbrin are similar, consistent with a trapping between the tighter bundles along the long axis of the myosin minifilament in both of these bundles. The relative angle distribution for α-actinin also agrees with a previously reported data set[46].

In contrast, the motor transport on fascin-crosslinked bundles shows a strong directional component, as evidenced by the peak at $\theta = 0$ in the relative angle distribution. Since fascin arranges actin filaments into polarity sorted bundles, this is likely due to directed movement along a bundle. The loose bundles created by filamin result in a nearly flat angular distribution with only small peaks at $\theta = 0$ and π. This indicates transport dominated by diffusion with only small directional components and few reversals.

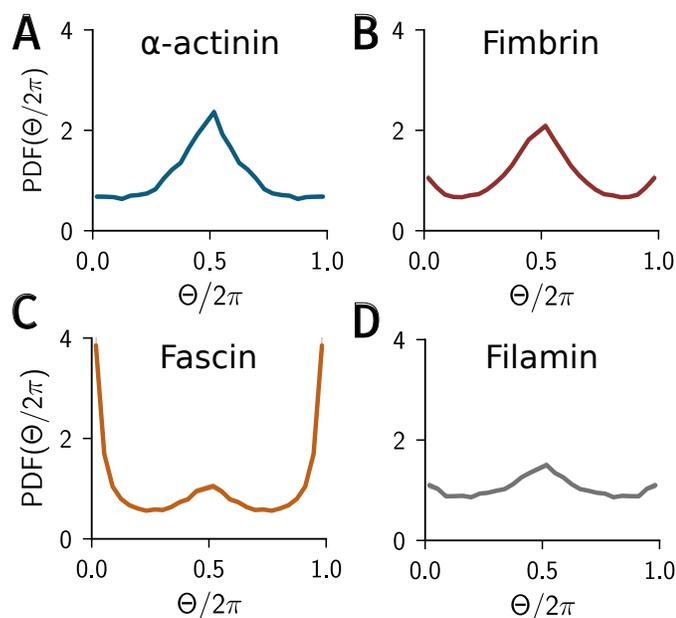Interestingly, the time-averaged mean-squared displacement

Fig. 3 Relative angle distributions of myosin II motor trajectories on actin networks crosslinked with either α-actinin (A), fimbrin (B), fascin (C) or filamin (D). A histogram of angles was created from each of the over 200 trajectories per condition by binning the angles $\Theta(\Delta)$ in 15 bins from [0, π].The resulting histogram was mirrored to create a range from [0, 2π] and then normalized such that the area under the curve is one. The line shown in the figure represents the average across trajectories and has the properties of a probability density function (PDF). See the main text for discussion of the choice of Δ.

shows a super-diffusive behavior for transport on the filamin-crosslinked network (Fig. 2A). Therefore, over large timescales the motor exhibits directed motion along the filamin network. However, on the smaller timescale used to calculate the angular distribution the motor shows nearly diffusional behavior. This could support two hypotheses. One is that the motors frequently hop between filaments in different microscopic orientations, such that the motion resembles a biased random walk. The other possible hypothesis is that the motors are detaching and diffusing within the bundles. Taken together, these measurements show that the relative angle distribution is sensitive to the bundle structure and can distinguish bundle structures resulting from different crosslinking proteins.

Conclusion

Using motor trajectories obtained from tracking myosin II motors moving on reconstituted bundled actin networks, we find that transport depends on the microscopic structure of the filament bundles. Intuitively, polarity-sorted bundles lead to directional transport, whereas mixed polarity bundles result in a combination of directed motion and trapped motion. Since the motor complex has a finite "reach," the loose bundles formed by filamin are less effective at trapping the motor than the tightly spaced fimbrin bundles. From our results, one can deduce the dynamics on a hypothetical actin network with wide filament spacing but polarity-sorted bundles. Our results suggest that the resulting motion would have a strong forward-directed component, but no sig-

nificant trapping, thus resulting in apparently persistent dynamics over short timescales and simple diffusion over long timescales.

In our experiments, the motors are in actin networks with quasi-two-dimensional geometries that have heights comparable to the thickness of the actin cortex *in vivo* [55,56]. The crosslinkers influence both the local bundle structure as well as the network architecture. The model bundles we construct here are composed of crosslinkers found in cellular bundles such as stress fibers and filapodia. We expect that in a three-dimensional network, or the actin cortex in cells which are composed of other proteins, the density of intersections between bundles would be different, which would affect the large scale network architecture and long-range transport properties. However, we focused our analysis on the short-timescale dynamics of the motors, which are dominated by intrabundle properties. We thus do not expect our results to be sensitive to the dimension of the material.

Our results have implications for the regulation of transport in cells, but are especially relevant for secreting cells, such as pancreatic beta cells. Although traditionally associated with microtubule-based transport, insulin secretory vesicles in beta cells have to cross the actin cortex before fusing with the membrane to release the hormone into the bloodstream [45]. The actin cortex is remodeled in response to insulin signaling [57]. It is likely that the timing of insulin release is affected by the structure of the actin cortex, and that the reported actin remodeling serves the purpose of making the network more amenable for traversing granules [58].

In summary, our results show that the organization of cytoskeletal networks has not only mechanical, but also dynamical consequences. The prevalence of different crosslinking proteins in different cellular regions, such as fillopodia, lamellopodia, or the cell cortex, could also be optimized for the transport processes that occur in those regions. Further studies should investigate the role of crosslinking proteins on motor dynamics *in vivo*. The principles that we elucidated could also be exploited to design novel materials with defined transport properties.

Acknowledgments

References

1 L. Blanchoin, R. Boujemaa-Paterski, C. Sykes and J. Plastino, *Physiological Reviews*, 2014, **94**, 235–263.

2 E. S. Chhabra and H. N. Higgs, *Nature Cell Biology*, 2007, **9**, 1110–1121.

3 T. M. Gomez and P. C. Letourneau, *Journal of Neuroscience*, 1994, **14**, 5959–5972.

4 C. Cyron, K. Müller, K. Schmoller, A. Bausch, W. Wall and R. Bruinsma, *EPL (Europhysics Letters)*, 2013, **102**, 38003.

5 S. L. Freedman, G. M. Hocky, S. Banerjee and A. R. Dinner, *Soft matter*, 2018, **14**, 7740–7747.

6 J. D. Winkelman, C. Suarez, G. M. Hocky, A. J. Harker, A. N. Morganthaler, J. R. Christensen, G. A. Voth, J. R. Bartles and D. R. Kovar, *Current Biology*, 2016, **26**, 2697–2706.

7 C. Suarez and D. R. Kovar, *Nature Reviews Molecular Cell Biology*, 2016, **17**, 799.

8 G. H. Koenderink and E. K. Paluch, *Current Opinion in Cell Biology*, 2018, **50**, 79–85.

9 E. M. Reichl, Y. Ren, M. K. Morphew, M. Delannoy, J. C. Effler, K. D. Girard, S. Divi, P. A. Iglesias, S. C. Kuo and D. N. Robinson, *Current Biology*, 2008, **18**, 471–480.

10 K. Schmoller, O. Lieleg and A. Bausch, *Physical Review Letters*, 2008, **101**, 118102.

11 O. Lieleg, M. M. Claessens and A. R. Bausch, *Soft Matter*, 2010, **6**, 218–225.

12 T. P. Stossel, J. Condeelis, L. Cooley, J. H. Hartwig, A. Noegel, M. Schleicher and S. S. Shapiro, *Nature Reviews Molecular Cell Biology*, 2001, **2**, 138.

13 J. Stricker, T. Falzone and M. L. Gardel, *Journal of biomechanics*, 2010, **43**, 9–14.

14 A.-C. Reymann, R. Boujemaa-Paterski, J.-L. Martiel, C. Guérin, W. Cao, H. F. Chin, M. Enrique, M. Théry and L. Blanchoin, *Science*, 2012, **336**, 1310–1314.

15 H. Ennomani, G. Letort, C. Guérin, J.-L. Martiel, W. Cao, F. Nédélec, M. Enrique, M. Théry and L. Blanchoin, *Current Biology*, 2016, **26**, 616–626.

16 S. Stam, S. L. Freedman, S. Banerjee, K. L. Weirich, A. R. Dinner and M. L. Gardel, *Proceedings of the National Academy of Sciences*, 2017, 201708625.

17 R. Rudolf, T. Salm, A. Rustom and H.-H. Gerdes, *Molecular Biology of the Cell*, 2001, **12**, 1353–1365.

18 M. Oheim and W. Stühmer, *European Biophysics Journal*, 2000, **29**, 67–89.

19 A. T. Lombardo, S. R. Nelson, M. Y. Ali, G. G. Kennedy, K. M. Trybus, S. Walcott and D. M. Warshaw, *Nature communications*, 2017, **8**, 15692.

20 J. P. Bergman, M. J. Bovyn, F. F. Doval, A. Sharma, M. V. Gudheti, S. P. Gross, J. F. Allard and M. D. Vershinin, *Proceedings of the National Academy of Sciences*, 2018, **115**, 537–542.

21 A. T. Lombardo, S. R. Nelson, G. G. Kennedy, K. M. Trybus, S. Walcott and D. M. Warshaw, *Proceedings of the National Academy of Sciences*, 2019, **116**, 8326–8335.

22 M. Scholz, S. Burov, K. L. Weirich, B. J. Scholz, S. A. Tabei, M. L. Gardel and A. R. Dinner, *Physical Review X*, 2016, **6**, 011037.

23 D. Ando, N. Korabel, K. C. Huang and A. Gopinathan, *Biophysical Journal*, 2015, **109**, 1574–1582.

24 S. Nagy, B. L. Ricca, M. F. Norstrom, D. S. Courson, C. M. Brawley, P. A. Smithback and R. S. Rock, *Proceedings of the National Academy of Sciences USA*, 2008, **105**, 9616–9620.

25 L. Conway, M. W. Gramlich, S. Ali Tabei and J. L. Ross, *Cytoskeleton*, 2014, **71**, 595–610.

26 J. Howard, *Mechanics of motor proteins and the cytoskeleton*,

Sinauer associates Sunderland, MA, 2001.

27 R. TyleráMcLaughlin *et al.*, *Soft Matter*, 2016, **12**, 14–21.

28 R. Mallik, A. K. Rai, P. Barak, A. Rai and A. Kunwar, *Trends in Cell Biology*, 2013, **23**, 575–582.

29 E. B. Krementsova, K. Furuta, K. Oiwa, K. M. Trybus and M. Y. Ali, *Journal of Biological Chemistry*, 2017, jbc–M117.

30 J. A. Spudich and S. Watt, *Journal of Biological Chemistry*, 1971, **246**, 4866–4871.

31 S. S. Margossian and S. Lowey, *Methods in enzymology*, Elsevier, 1982, vol. 85, pp. 55–71.

32 A. B. Verkhovsky and G. G. Borisy, *Journal of Cell Biology*, 1993, **123**, 637–652.

33 S. W. Craig, C. L. Lancashire and J. A. Cooper, *Methods in enzymology*, Elsevier, 1982, vol. 85, pp. 316–321.

34 D. Vignjevic, D. Yarar, M. D. Welch, J. Peloquin, T. Svitkina and G. G. Borisy, *Journal of Cell Biology*, 2003, **160**, 951–962.

35 C. T. Skau and D. R. Kovar, *Current Biology*, 2010, **20**, 1415–1422.

36 Y. Li, J. R. Christensen, K. E. Homa, G. M. Hocky, A. Fok, J. A. Sees, G. A. Voth and D. R. Kovar, *Molecular Biology of the Cell*, 2016, **27**, 1821–1833.

37 K. L. Weirich, J. N. Israelachvili and D. K. Fygenson, *Biophysical Journal*, 2010, **98**, 85–92.

38 D. B. Allan, T. A. Caswell and N. C. Keim, *Trackpy v0.2*, 2014, http://dx.doi.org/10.5281/zenodo.9971.

39 M. P. Murrell and M. L. Gardel, *Proc. Natl. Acad. Sci. USA*, 2012, **109**, 20820–20825.

40 K. A. Taylor and D. W. Taylor, *Biophysical Journal*, 1994, **67**, 1976–1983.

41 O. Pelletier, E. Pokidysheva, L. S. Hirst, N. Bouxsein, Y. Li and C. R. Safinya, *Physical Review Letters*, 2003, **91**, 148102.

42 A. Bretscher, *Proceedings of the National Academy of Sciences*, 1981, **78**, 6849–6853.

43 J. R. Bartles, *Current Opinion in Cell Biology*, 2000, **12**, 72–78.

44 F. Nakamura, T. P. Stossel and J. H. Hartwig, *Cell Adhesion & Migration*, 2011, **5**, 160–169.

45 S. A. Tabei, S. Burov, H. Y. Kim, A. Kuznetsov, T. Huynh, J. Jureller, L. H. Philipson, A. R. Dinner and N. F. Scherer, *Proceedings of the National Academy of Sciences*, 2013, **110**, 4911–4916.

46 S. Burov, S. A. Tabei, T. Huynh, M. P. Murrell, L. H. Philipson, S. A. Rice, M. L. Gardel, N. F. Scherer and A. R. Dinner, *Proceedings of the National Academy of Sciences USA*, 2013, **110**, 19689–19694.

47 A. V. Weigel, B. Simon, M. M. Tamkun and D. Krapf, *Proceedings of the National Academy of Sciences USA*, 2011.

48 I. Golding and E. C. Cox, *Physical Review Letters*, 2006, **96**, 098102.

49 Tolić-Norrelykke, Iva Marija and Munteanu, Emilia-Laura and Thon, Genevieve and Oddershede, Lene and Berg-Sorensen, Kirstine, *Physical Review Letters*, 2004, **93**, 078102.

50 S. Weber, A. Spakowitz and J. Theriot, *Physical Review Letters*, 2010, **104**, 238102.

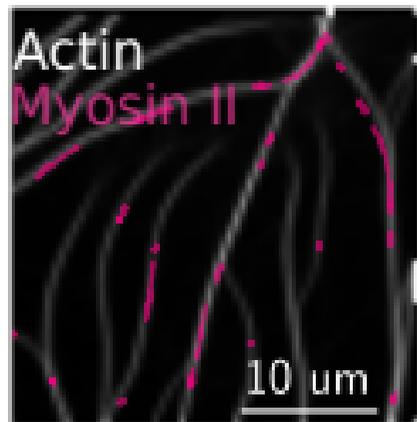51 J. A. Spudich, S. J. Kron and M. P. Sheetz, *Nature*, 1985, **315**,

584–586.

52 S. J. Kron and J. A. Spudich, *Proceedings of the National Academy of Sciences*, 1986, **83**, 6272–6276.

53 M. J. Müller, S. Klumpp and R. Lipowsky, *Proceedings of the National Academy of Sciences USA*, 2008, **105**, 4609–4614.

54 W. O. Hancock, *Nat. Rev. Mol. Cell Biol.*, 2014, **15**, 615–628.

55 P. Chugh, A. G. Clark, M. B. Smith, D. A. Cassani, K. Dierkes, A. Ragab, P. P. Roux, G. Charras, G. Salbreux and E. K. Paluch, *Nature cell biology*, 2017, **19**, 689.

56 A. G. Clark, K. Dierkes and E. K. Paluch, *Biophysical journal*, 2013, **105**, 570–580.

57 R. Tunduguru, T. T. Chiu, L. Ramalingam, J. S. Elmendorf, A. Klip and D. C. Thurmond, *Biochemical pharmacology*, 2014, **92**, 380–388.

58 C. Arous and P. A. Halban, *American Journal of Physiology-Endocrinology and Metabolism*, 2015, **309**, E611–E620.

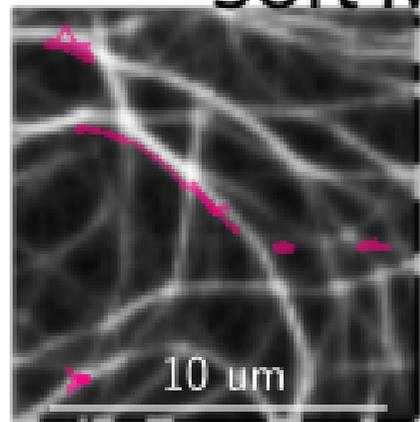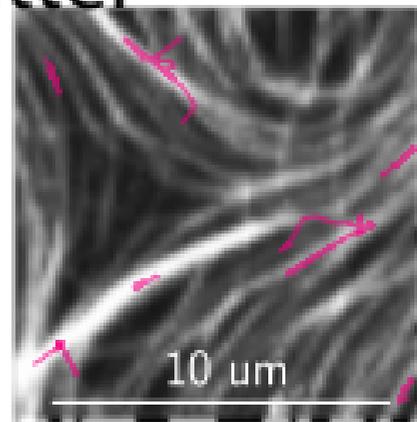Filamin   α-actinin   Fimbrin   Fascin